Heliyon 7 (2021) e06044

Contents lists available at ScienceDirect

Heliyon

journal homepage: www.cell.com/heliyon

Research article

^{1}H and ^{13}C NMR chemical shifts of 2-*n*-alkylamino-naphthalene-1,4-diones

Rishikesh Patil [a], Mahesh Jadhav [a], Sunita Salunke-Gawali [a,*], Dipali N. Lande [a], Shridhar P. Gejji [a], Debamitra Chakravarty [b]

[a] Department of Chemistry, Savitribai Phule Pune University, Pune, 411007, Maharashtra State, India
[b] Central Instrumentation Facility, Savitribai Phule Pune University, Pune, 411007, Maharashtra State, India

ARTICLE INFO

Keywords:
Naphthoquinone
Aminonaphthoquinone
Chemical shift
2D NMR

ABSTRACT

^{1}H as well as ^{13}C chemical shifts of 32 compounds of C (3) substituted 2-(*n*-alkylamino)-3R-naphthalene-1,4-dione (where *n*-alkyl: methyl, to octyl, R = H, Cl, Br, and CH_3) are investigated through ^{1}H, ^{13}C, DEPT, gDQCOSY, and gHSQCAD NMR experiments and M06-2X/6-311++G (d,p) density functional theory are discussed. Single crystal X-ray structure of Br-3, as well as 18 different derivatives of naphthalene-1,4-diones, are revealed for its inter and intra-molecular hydrogen bonding interactions.

1. Introduction

Annamycin antibiotics with aminonaphthoquione in its core include naphthomycin K, divergolides C and divergolide D, naphthomycin A [1, 2, 3, 4]. Annamycin antibiotic finds applications in treating tuberculosis, leprosy, and AIDS-related mycobacterial infections. Aminonaphthoquinones Echimamine A, Echinamine B, and Spinamine are isolated from natural resources [5, 6, 7, 8]. Aminonaphthoquinone antibiotics are synthesized in the laboratory [8]. More interestingly, naphthalene-1,4-dione is rendered with anticancer, antibacterial, antifungal activities [9, 10, 11, 12, 13, 14, 15, 16] and its derivatives Menadione, Juglone, Plumbagin, or Vitamin K3-epoxide find applications in therapeutic use. These drug molecules generate reactive oxygen species (ROS), cause cell growth inhibition and consequently, cell death [17, 18, 19]. It has been realized that the effective stabilization of the enol species in naphthalene-1,4-dione derivatives that participate in electron transfer processes is key to cell growth inhibition [20].

The insights for structural rearrangements at the molecular level are crucial for understanding the biological activity. Thus their ramifications to spectral features have been the focus of attention for quite some time. To this direction, Illos et al. studied the fluorescence switching of molecular naphthoquinone, which showed chemo-as well as electro photoswitching. Furthermore, the effect of varying redox control, spacers, and fluorophore subunits on fluorescent molecules' switching behavior has also been investigated [21]. It has been inferred that the π-conjugated electrons make naphthalene-1,4-diones a probable candidate for nonlinear optical (NOL) properties. Mande et al. have carried out a detailed study on the NOL properties of naphthalene-1,4-diones derivatives employing the density functional theory (DFT) and Z-scan technique [22]. More recently, Navarro-Gracia et al. explored the naphthalene-1,4-dione derivatives as sensors in supramolecular chemistry to recognize anions [23].

In pursuance of the above studies, it has further been shown that the spectroscopy techniques unravel structural arrangements accompanying the naphthalene-1,4-dione derivatives using the chemical shifts data obtained from the ^{1}H and ^{13}C NMR experiments. The substituted positions in different isomers thus can be distinguished. Ribeiro et al. investigated 1,2- and naphthalene-1,4-dione derivatives. These groups established that the end group's ortho/para position and size attached to the naphthoquinone ring [24] could be ascertained through the chemical shifts measured from the experiment.

* Corresponding author.
E-mail address: sunita_salunke@rediffmail.com (S. Salunke-Gawali).

https://doi.org/10.1016/j.heliyon.2021.e06044
Received 20 June 2020; Received in revised form 29 September 2020; Accepted 18 January 2021

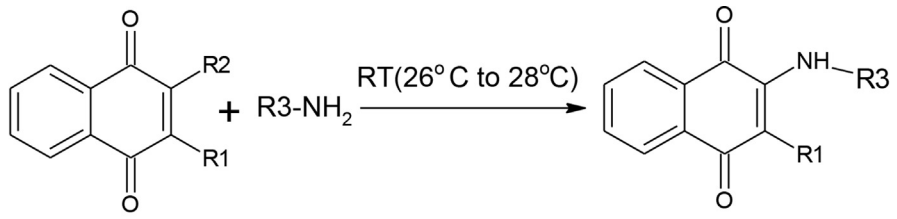

R1 = H(H-1 to H-8), CH_3 (M-1 to M-8), Br(Br-1 to Br-8), Cl(Cl1- to Cl-8)

R2 = H, Br, Cl

R3 = -CH_3(1), -C_2H_5(2), -C_3H_7(3), -C_4H_9(4), -C_5H_{11}(5), -C_6H_{13}(6), -C_7H_{15}(7), -C_8H_{17}(8)

Scheme 1. Synthesis of *n*-alkylamino derivatives of naphthalene-1,4-dione.

a)

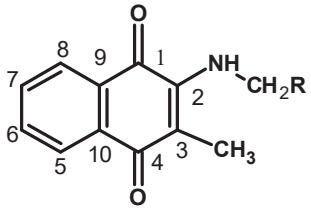

where,

M-1: R=H ; M-2: R=CH_3;

M-3:R=C_2H_5, M-4: R=C_3H_7

M-5: R=C_4H_9; M-6: R=C_5H_{11};

M-7: R=C_6H_{13}; M-8: R=C_7H_{15}

b)

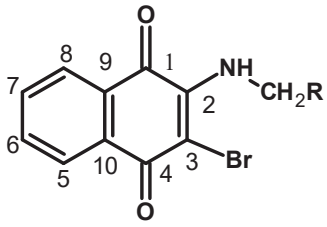

where,

Br-1: R=H ; Br-2: R=CH_3;

Br-3:R=C_2H_5, Br-4: R=C_3H_7

Br-5: R=C_4H_9; Br-6: R=C_5H_{11};

Br-7: R=C_6H_{13}; Br-8: R=C_7H_{15}

c)

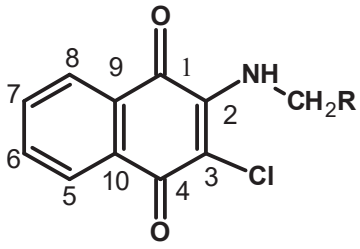

where,

Cl-1: R=H ; Cl-2: R=CH_3;

Cl-3:R=C_2H_5, Cl-4: R=C_3H_7

Cl-5: R=C_4H_9; Cl-6: R=C_5H_{11};

Cl-7: R=C_6H_{13}; Cl-8: R=C_7H_{15}

d)

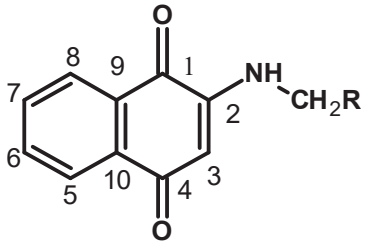

where,

H-1: R=H ; H-2: R=CH_3;

H-3:R=C_2H_5, H-4: R=C_3H_7

H-5: R=C_4H_9; H-6: R=C_5H_{11};

H-7: R=C_6H_{13}; H-8: R=C_7H_{15}

Figure 1. Molecular structures a) 2-(*n*-alkylamino)-3-methyl-naphthalene-1,4-dione, b) 2-(*n*-alkylamino)-3-bromo-naphthalene-1,4-dione, c) 2-(*n*-alkylamino)-3-chloro-naphthalene-1,4-dione and d) 2-(*n*-alkylamino)-naphthalene-1,4-dione.

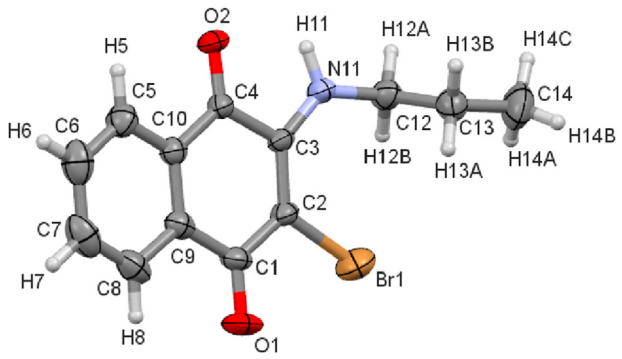

Figure 2. ORTEP diagram Br-3. The ellipsoids are drawn with 50% probability.

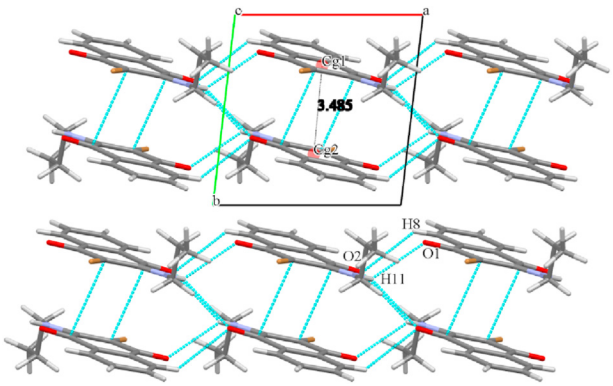

Figure 3. Molecular packing of Br-3 down a-axis.

Furthermore, Bedir et al. analyzed the structure typifying B-Lapachone naphthoquinone that revealed the ortho-coupled hydrogen from the ^{1}H NMR experiments.

Moreover, the stereochemistry of lapachone was elucidated through the NMR data [25]. Consequently, 1D and 2D NMR data on naphthoquinone derivatives isolated via chloroform extraction of Diospyros maritime BLUME (Ebenaceae) fruit were measured. Subsequently ^{1}H and ^{13}C NMR signals were assigned. Higa et al. studied the quinonoid protons' signals, and correlated to heteronuclear multiple bond connectivity (HMBC), thereby specified the position of dimeric linkage in the synthesized molecule [26]. To probe further into the conformer, Prezhdo et al. studied the Kerr effect and the ^{1}H as well as ^{13}C NMR spectra of chloroalkyl derivatives of naphthalene-1,4-dione [27].

As pursuance to the above considerations, we in the present work undertake synthesis and characterization of a series of 2-(*n*-alkylamino)-3-R-naphthalene-1,4-dione (the *n*-alkyl group being methyl to octyl) [28, 29, 30, 31, 32, 33, 34]; as shown in Scheme 1.

All aminonaphthoquinone derivatives were characterized by using various spectroscopic experiments, namely, NMR, FTIR, UV-visible, and elemental analysis. The work focuses on ^{1}H and ^{13}C chemical shifts and substituent effects on chemical shifts. Consequently, the 2D NMR data further demonstrate the impact of substituent electronegativity on chemical shifts along with the methyl (-CH_3, M-1 to M-8), bromo (-Br, Br-1 to Br-8), chloro (-Cl, Cl-1 to Cl-8) series, which are depicted in Figure 1 along with unsubstituted (-H in H-1 to H-8).

Table 1. Crystal data and structure refinement for Br-3.

Empirical formula	C_{13} H_{12} Br N O_2	
Formula weight	294.15	
Temperature	296 (2) K	
Wavelength	0.71073 Å	
Crystal system	Triclinic	
Space group	*P -1*	
Unit cell dimensions	a = 7.3470 (2) Å	α = 110.3660 (6)°
	b = 7.9862 (2) Å	β = 91.5200 (6)°
	c = 10.9580 (2) Å	γ = 95.6780 (6)°
Volume	598.52 (2) $Å^3$	
Z	2	
Density (calculated)	1.632 Mg/m^3	
Absorption coefficient	3.422 mm^{-1}	
F (000)	296	
Crystal size	0.32 × 0.26 × 0.11 mm^3	
Theta range for data collection	2.759–28.474°	
Index ranges	-9<=h<=9, -10<=k<=10, -14<=l<=14	
Reflections collected	24055	
Independent reflections	3019 [R (int) = 0.0630]	
Completeness to theta = 25.242°	99.9 %	
Absorption correction	Semi-empirical from equivalents	
Max. and min. transmission	0.686 and 0.358	
Refinement method	Full-matrix least-squares on F^2	
Data/restraints/parameters	3019/0/155	
Goodness-of-fit on F^2	1.037	
Final R indices [I > 2 sigma(I)]	R1 = 0.0580, wR2 = 0.1615	
R indices (all data)	R1 = 0.0792, wR2 = 0.1751	
Extinction coefficient	n/a	
Largest diff. peak and hole	0.636 and -0.578 e.$Å^{-3}$	

Table 2. X-ray structure data of *n*-alkylamino-3R-naphthalene-1,4-diones.

Compound	Space group	CCDC	N–H···O	C–H···O	Cl···π/π···π	Bifurcated hydrogen through O(1)/O(4)
Cl-1	*P -1*	907096	√	√	π···π	O(1), O(4)
Cl-2	*Pca2$_1$*	907097	√	√	Cl···π	-
Cl-3	*P-1*	907098	√	√	π···π	O(1)
Cl-4	*P2$_1$*	925343	√	√	π···π/Cl···π	O(4)
Cl-6	*P2$_1$/C*	925344	√	√	C–H···π	-
Cl-8	*P2$_1$/C*	924571	√	√	π···π	-
Br-3	*P-1*	949769	√	√	π···π	O(4)
Br-2	*P c a 2$_1$*	953429	√	×	Br···π	-
M-1	*C2/C*	640771	√	√	C–H···π/π···π	O(1)/O(4)
M-2	*C2/C*	1446868	√	√	C–H···π	O(4)
M-3	*P1*	1021052	√	√	π···π	O(4)
M-6	*P2$_1$*	1446870	√	√	C–H···π	O(4)
H-2	*P2$_1$/C*	975344	√	√	-	O(4)
H-3	*P2$_1$/C*	1417468	√	√	π···π	O(1)/O(4)
H-4	*P-1*	1426148	√	√	π···π	O(4)
H-6	*P-1*	975345	√	√	C···O, C···N	-
H-8	*P-1*	1417469	√	√	C···O	-

Table 3. ^{1}H chemical shift in ppm (observed and calculated) of H-1, M-1, Br-1, Cl-1.

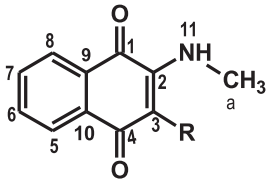

R = H; H-1, CH_3; M-1, Br; Br-1, Cl; Cl-1

	Experimental				Theoretical			
	H-1	M-1	Br-1	Cl-1	H-1	M-1	Br-1	Cl-1
H (8)	7.94	7.90	7.95	7.96	9.96	10.14	9.51	9.96
H (7)	7.80	7.74	7.79	7.81	9.70	9.33	9.46	8.94
H (6)	7.69	7.64	7.71	7.72	9.61	9.46	9.84	9.21
H (5)	7.91	7.84	7.94	7.95	9.61	9.90	10.02	10.23
R-(3)	5.56	2.10	-	-	7.22	4.03	-	-
NH	7.60	6.83	7.53	7.55	6.16	6.05	6.37	6.37
H(a)	2.76	3.14	3.25	3.28	3.72	3.26	4.33	4.36

2. Experimental section

2.1. Materials and methods

The materials used for synthesis, vitamin K3 (2-methyl-naphthalene-1,4-dione), 2,3-dichloro-naphthalene-1,4-dione, 2,3-dibromonaphthalene-1,4-dione, naphthalene-1,4-dione, ethanamine solution (70%), propan-1-amine (99%), butan-1-amine (99%), pentyl-1-amine (99%), hexan-1-amine (99%), heptan-1-amine (99%) and octan-1-amine(99%) were purchased from Sigma-Aldrich and used as received. Methylamine solution (40%), obtained from Loba chemicals; toluene and methanol obtained from Merck Chemicals. Solvents were distilled by standard methods [30,35] and dried wherever necessary.

2.2. Synthesis

All compounds were synthesized and characterized using reported procedures as described in references [27, 28, 29, 30, 31, 32, 33]. 1 g of 2-methyl-naphthalene-1,4-dione (5.80 mmol for M-1 to M-8), 2,3-dibromonaphthalene-1,4-dione (3.2 mmol for Br-1 to Br-8), 2, 3-dichloro-naphthalene-1,4-dione (4.4 mmol for Cl-1 to Cl-8), naphthalene-1,4-dione (6.32 mmol for H-1 to H-8) dissolved in 25–30 ml of dichloromethane and magnetically stirred at room temperature (26 °C–28 °C). The respective *n*-alkylamines (methyl - octyl) in equal mmol to that of parent naphthoquinone was added directly to this solution [28,36, 37, 38]. The mixture was magnetically stirred for 24 h. The solvent was evaporated naturally. With column chromatography, the

Table 4. ^{1}H chemical shift in ppm (observed and theoretical) of H-4, M-4, Br-4 and Cl-4.

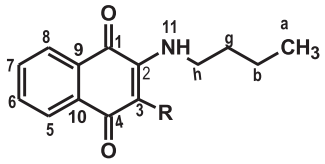

R = H; H-4, CH_3; M-4, Br; Br-4, Cl; Cl-4

	Experimental				Theoretical			
	H-4	M-4	Br-4	Cl-4	H-4	M-4	Br-4	Cl-4
H (8)	7.90	7.86	7.97	7.88	10.05	10.12	10.08	10.22
H (7)	7.76	7.74	7.80	7.66	9.60	9.32	9.37	9.42
H (6)	7.65	7.65	7.73	7.53	9.42	9.57	9.48	9.56
H (5)	7.89	7.88	7.95	7.77	9.55	9.58	9.70	6.67
R-(3)	5.64	2.06	-		7.01	3.31		
NH	7.50	6.49	7.42	7.80	6.03	5.83	6.28	6.25
H(a)	0.88	0.84	0.89	0.86	2.05	1.93	2.07	2.07
H(b)	1.33	1.27	1.33	1.32	2.28	2.21	2.37	2.30
H(g)	1.54	1.48	1.59	1.52	2.62	2.51	2.38	2.50
H(h)	3.15	3.45	3.74	2.79	3.88	4.25	4.79	4.82

Table 5. ^{1}H chemical shift in ppm (observed and theoretical) of H-8, M-8, Br-8 and Cl-8.

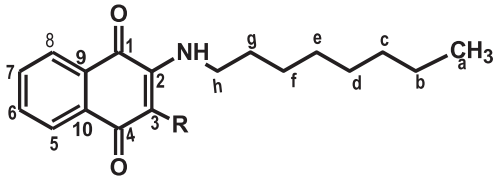

R = H; H-8, CH_3; M-8, Br; Br-8, Cl; Cl-8

	Experimental				Theoretical			
	H-8	M-8	Br-8	Cl-8	H-8	M-8	Br-8	Cl-8
H (8)	7.96	7.92	7.96	7.97	10.18	10.26	9.99	10.06
H (7)	7.81	7.76	7.79	7.80	9.67	9.03	9.15	9.31
H (6)	7.70	7.67	7.72	7.73	9.53	9.25	9.26	9.66
H (5)	7.92	7.86	7.95	7.95	9.29	9.52	10.15	9.88
R-(3)	5.64	2.05	-		7.04	3.25	-	-
NH	7.53	6.60	7.46	7.43	6.08	5.96	6.37	6.08
H(a)	0.83	0.82	0.82	0.83	1.85	1.84	1.88	1.81
H(b)	1.24	1.25	1.24	1.27	2.09	2.16	2.11	2.15
H(c)	1.24	1.25	1.24	1.27	2.18	2.20	2.34	2.12
H(d)	1.24	1.25	1.24	1.27	2.31	2.29	2.21	2.29
H(e)	1.24	1.25	1.24	1.27	2.38	2.39	2.36	2.29
H(f)	1.24	1.25	1.24	1.27	2.39	2.33	2.50	2.33
H(g)	1.56	1.54	1.58	1.59	2.73	2.66	2.64	2.46
H(h)	3.14	3.51	3.70	3.72	3.95	4.52	4.86	4.67

Table 6. ^{13}C chemical shift in ppm of H-1, M-1, Br-1, Cl-1.

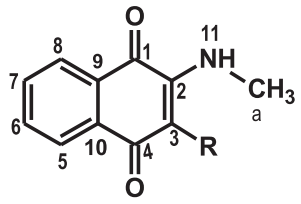

R = H; H-1, CH_3; M-1, Br; Br-1, Cl; Cl-1

Experimental	H-1	M-1	Br-1	Cl-1
C1	181.44	181.53	175.00	175.15
C2	149.50	147.56	148.29	146.07
C3	99.18	109.89	129.96	108.05
C4	181.10	182.22	179.94	180.15
C5	125.35	134.22	125.96	125.67
C6	132.07	126.23	133.00	132.46
C7	134.77	134.53	134.75	134.78
C8	125.82	126.89	126.50	126.34
C9	133.28	130.71	131.82	129.84
C10	130.55	131.96	131.82	132.06
C12	-	10.44	-	-
a	28.57	32.40	32.79	32.25

Table 7. ^{13}C chemical shift in ppm of H-4, M-4, Br-4, and Cl-4.

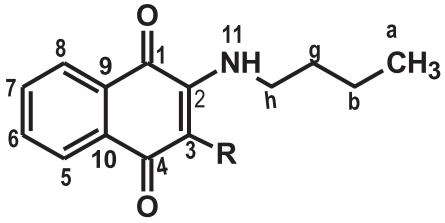

R = H; H-4, CH_3; M-4, Br; Br-4, Cl; Cl-4

Experimental	H-4	M-4	Br-4	Cl-4
C1	181.55	181.59	175.08	173.50
C2	149.48	146.70	147.28	166.76
C3	99.15	110.59	129.81	112.68
C4	181.16	182.26	179.80	184.32
C5	125.28	125.63	126.52	125.21
C6	132.04	132.78	132.49	135.08
C7	134.76	134.45	134.77	133.62
C8	125.82	125.38	126.01	125.42
C9	133.19	130.25	131.74	130.47
C10	130.36	132.09	131.74	130.57
C12	-	10.66	-	-
g	29.37	32.76	32.65	29.09
b	19.68	19.38	19.26	19.07
a	13.62	13.73	13.65	13.45
h	41.57	44.14	43.82	38.64

Table 8. ^{13}C chemical shift in ppm of H-8, M-8, Br-8, and Cl-8.

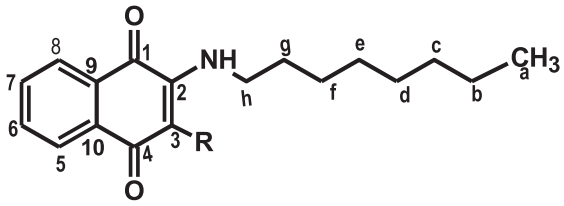

R = H; H-8, CH_3; M-8, Br; Br-8, Cl; Cl-8

Experimental	H-8	M-8	Br-8	Cl-8
C1	181.57	181.56	175.11	175.14
C2	148.48	146.65	147.30	164.55
C3	99.12	110.59	129.85	129.91
C4	181.13	182.24	179.86	179.89
C5	125.27	125.59	126.57	126.59
C6	132.05	132.05	132.52	132.56
C7	134.78	134.78	134.81	134.83
C8	125.82	125.35	126.03	126.05
C9	133.20	130.26	131.77	131.79
C10	130.37	132.78	131.77	131.79
C12		10.63		
f	28.65	26.10	25.98	25.99
e	28.58	28.67	28.58	28.56
d	27.22	28.62	28.62	28.63
c	26.44	31.20	31.16	31.18
g	31.18	30.58	30.51	30.53
b	22.03	22.08	22.04	22.06
a	13.90	13.93	13.90	13.93
h	41.83	44.41	44.05	44.07

crude solid product was purified using toluene: methanol (9:1) as an eluent system. Pure solid products were finally obtained with 60 %–80%. Yield following the reduction of the pure fraction with the rotatory evaporator.

2.3. Analytical methods

Varian Mercury 500 MHz NMR spectrometer was used to record ^1H, ^{13}C, DEPT, gDQCOSY, and gHSQCAD NMR of all compounds in DMSO-d_6 with TMS (tetramethylsilane) as a reference.

2.4. X-ray crystal structure

X-ray data of Br-3 was collected on D8 Venture PHOTON 100 CMOS diffractometer using graphite monochromatized Mo-Kα radiation (λ = 0.7107 Å) with exposure/frame = 10 s. The X-ray generator was operated at 50 kV and 30 mA, an initial set of cell constants and an orientation matrix calculated from 24 frames. The optimized strategy used for data collection included different sets off, and ω scans with 0.5° steps in φ/ω. Crystal to detector distance was 5.00 cm with 512 × 512 pixels/frame, Oscillation/frame -0.5°, maximum detector swing angle = -30.0°, beam

Table 9. Experimental ^1H chemical shift in ppm of Br-1 to Br-8.

	Br -1	Br -2	Br -3	Br -4	Br -5	Br -6	Br -7	Br -8
H (8)	7.95	7.97	7.97	7.97	7.96	7.90	7.98	7.96
H (7)	7.79	7.80	7.80	7.80	7.80	7.77	7.79	7.79
H (6)	7.71	7.72	7.72	7.73	7.72	7.68	7.72	7.72
H (5)	7.94	7.95	7.95	7.95	7.95	7.92	7.96	7.95
NH	7.53	7.43	7.44	7.42	7.42	7.44	7.43	7.46
H(a)	3.25	1.20	0.88	0.89	0.86	0.82	0.84	0.82
H(b)	-	-	-	1.33	1.30	1.23	1.28	1.24
H(c)	-	-	-	-	1.30	1.23	1.28	1.24
H(d)	-	-	-	-	-	1.23	1.28	1.24
H(e)	-	-	-	-	-	-	1.28	1.24
H(f)	-	-	-	-	-	-	-	1.24
H(g)	-	-	1.62	1.59	1.60	1.56	1.61	1.58
H(h)	-	3.77	3.70	3.74	3.73	3.67	3.72	3.70

Table 10. Experimental ^{13}C chemical shift in ppm of Br-1 to Br-8.

	Br -1	Br -2	Br -3	Br -4	Br -5	Br -6	Br -7	Br -8
C1	175.00	175.60	175.13	175.08	175.09	175.08	175.12	175.11
C2	148.29	147.87	147.87	147.28	147.30	147.37	147.37	147.30
C3	129.96	130.38	129.87	129.81	129.85	129.84	129.85	129.85
C4	179.94	180.35	179.85	179.80	179.84	179.83	179.86	179.86
C5	125.96	126.50	126.04	126.52	126.03	126.54	126.02	126.57
C6	133.00	133.00	132.54	132.49	132.51	132.51	132.56	132.52
C7	134.75	135.26	134.80	134.77	134.81	134.78	134.80	134.81
C8	126.50	127.04	126.57	126.01	126.55	126.01	126.55	126.03
C9	131.82	132.24	131.76	131.74	131.76	131.75	131.77	131.77
C10	131.82	132.24	131.76	131.74	131.76	131.75	131.77	131.77
a	32.79	16.78	10.82	13.65	13.85	13.79	13.87	13.90
b	-	-	23.87	19.26	21.80	21.95	21.95	22.04
c	-	-	-	-	28.22	30.26	25.95	31.16
d	-	-	-	-	-	25.65	28.31	28.62
e	-	-	-	-	-	-	31.12	28.58
f	-	-	-	-	-	-	-	25.98
g	-	-	-	32.65	30.24	30.47	30.50	30.51
h	-	39.61	45.67	43.82	44.04	44.08	44.08	44.05

centre = (260.2, 252.5), in-plane spot width = 1.24. Data integration was carried out using the Bruker SAINT program, and empirical absorption correction for intensity data using Bruker SADABS. The program is integrated into the APEX II package [39]. The data corrected for Lorentz and polarization effects. The structure was solved by direct Method using the SHELX-97 [40] with the final refinement of the structure performed by a full-matrix least-squares technique with anisotropic thermal data for non-hydrogen atoms on F2. The non-hydrogen atoms refined anisotropically, while the hydrogen atoms refined at the calculated positions as riding atoms with isotropic displacement parameters [40]. Molecular diagrams are drawn by Mercury software [41]. SHELXTL [40] and PLATON [42] was used to perform the structural calculations of Br-3 [43].

3. Result and discussion

All 32 compounds (Figure 1) were synthesized and characterized [28, 29, 30, 31, 32, 33, 34]. Molecular structures of most of the derivatives revealed from single-crystal X-ray diffraction studies. The majority of these compounds possess biological activity, for example, antibacterial [30], antifungal [28], and antiproliferative activity [31,32, 34,44].

3.1. X-ray structure of Br-3

Crystal structures of 18 compounds (Table 2) of *n*-alkylamino-naphthalene-1,4-dione are known [28, 29, 30, 31, 32, 33, 34]. Compounds Cl-2 and Br-2 crystallize in the orthorhombic space group, whereas other compounds either crystallize in triclinic or monoclinic space groups. All solved crystal structures showed intramolecular and intermolecular N–H···O, C–H···O (except Br-2) interactions (Table 2). Besides, Cl-2, Cl-4 possess Cl···π and Br-2; Br···π interaction. The C–H···π interactions are evident in the methyl derivatives M-1, M-2, and M-6. Lastly, the H-3 and H-6 indicate the presence of C···O and N···O interactions.

ORTEP diagram of Br-3 is shown in Figure 2. The structure of Br-3 was reported at 100K, with a minor variation of cell parameters observed at 296 K (Table 1) with an increase in cell volume by 24 $Å^3$. The molecules of Br-3 showed inter and intramolecular N–H···O hydrogen bonding, and the molecules formed a polymeric chain via intermolecular C–H···O and N–H···O interactions. The neighboring polymeric chains are connected via bifurcated C–H···O, N–H···O, and π-π interactions (Figure 3). Other analogs further evidence bifurcated hydrogen bonding through either O(1) and O(4) (cf. Table 2).

3.2. NMR spectroscopy

NMR spectra of all the compounds with a series of side-chain homologated derivatives of 2-(*n*-alkylamino)-3R-naphthalene-1,4-dione (where the *n*-alkyl group is methyl to octyl) and different substituent at C(3) position $–CH_3$ (M-1 to M-8), or –Br (Br-1 to Br -8), or -Cl (Cl-1 to Cl-8), and –H(H-1 to H-8) have been analyzed from their NMR spectra, DMSO-d_6 used as a solvent. We have performed the analysis with a 1D experiment like ^1H, ^{13}C, and DEPT to compare every side chain derivative's chemical shifts with different substituents at C (3). ^1H, ^{13}C NMR of all compounds represented in Fig. S1 through Fig. S32 in ESI, and their gDQCOSY and gHSQCAD spectra are presented in Fig. S33 through Fig. S80 in ESI. The experimental and calculated ^1H chemical shift is shown in Table S1 through Table S8, whereas the ^{13}C chemical shift is presented in Table S9 through Table S16 in ESI. The representative ^1H chemical shifts of methyl, butyl, and octyl derivatives is shown in Tables 3, 4, and 5, respectively, and the ^{13}C chemical shifts are presented in Tables 6, 7 and 8, ^1H and ^{13}C chemical shift of Br-1 to Br-8 respectively shown in Tables 9 and 10.

Chemical shifts of all four homologated series of compounds obtained from the ^1H, ^{13}C NMR spectra have been compared.

^1H chemical shift of –NH- was observed at ~ δ = 7.5 ppm for H-1 to H-8, at ~ δ = 7.4 ppm for Br-1 to Br-8 (Table 9); however, it varied in Cl-1 to Cl-8 (at ~ δ = 7.4–7.5 ppm), and it revealed upfield shift near δ = 6.5 ppm in M-1 to M-8. The X-ray crystal structures of these compounds reveal intra and intermolecular N–H···O interactions. Besides, the C(3) substitution may affect the ^1H chemical shift of –NH-. The downfield ^1H chemical shift was noticed for the first member of each series (H-1, M-1, Cl-1, and Br-1). The singlet was observed to C(3)-H at ~ δ = 5.60 ppm for H-1 to H-8 and C(3)-methyl in M-1 to M-8 at ~ δ = 2.10 ppm. The

aromatic proton H(5) takes part intermolecular C–H···O interaction (Table 2) in most of the crystal structures of known derivatives; if such interactions exist in the solution, the chemical shift variation is expected. The ^{1}H chemical shift was observed at ~ δ = 7.8–7.9 ppm in all compounds; this implies that the intermolecular C–H···O interaction does not directly affect its chemical shift [45]. A similar inference for the ^{1}H chemical shift of other benzenoid ring protons H(8), H(6), and H(7) can be drawn. The chemical shift of terminal –CH_3 protons of the *n*-alkylamino chain was observed at ~ δ = 0.8 ppm, except for the methyl or ethyl series of compounds.

The differences for the ^{13}C chemical shift of C(1), C(2), C(3), and C(4) of the series are transparent. The chemical shift of C(1) and C(4) was observed at ~ δ = 181 ppm in H-1 to H-8, whereas for M-1 to M-8, it shows up at δ = 181 ppm and ~ δ = 182 ppm, respectively [46]. On the contrary, for the Cl-1 to Cl-8 and Br-1 to Br-8 (Table 10), the upfield shift was observed. The C (1) carbonyl carbon of the bromo (Br-1 to Br-8) and chloro (Cl-1 to Cl-8) series showed the carbon chemical shift at ~ δ = 174 ppm, whereas for proton (H-1 to H-8) and methyl (M-1 to M-8) series of compounds the shift in the chemical shift by ~ 7 ppm, i.e., at ~ δ = 181 ppm which ascertains the intramolecular hydrogen bonding between C–O–N–H is stronger in hydrogen (H-1 to H-8) and the methyl (M-1 to M-8) than in bromo (Br-1 to Br-8) and chloro (Cl-1 to Cl-8) series of compounds which can also noticed from by single-crystal X-ray diffraction studies [27, 28, 29, 30, 31, 32, 33]. ^{13}C chemical shift of C(2) showed up near δ = 149 ppm for H-1 to H-8 which reveal upfield shift for M-1 to M-8 (δ = 146 ppm) Br-1 to Br-8 (at ~ δ = 147 ppm). and

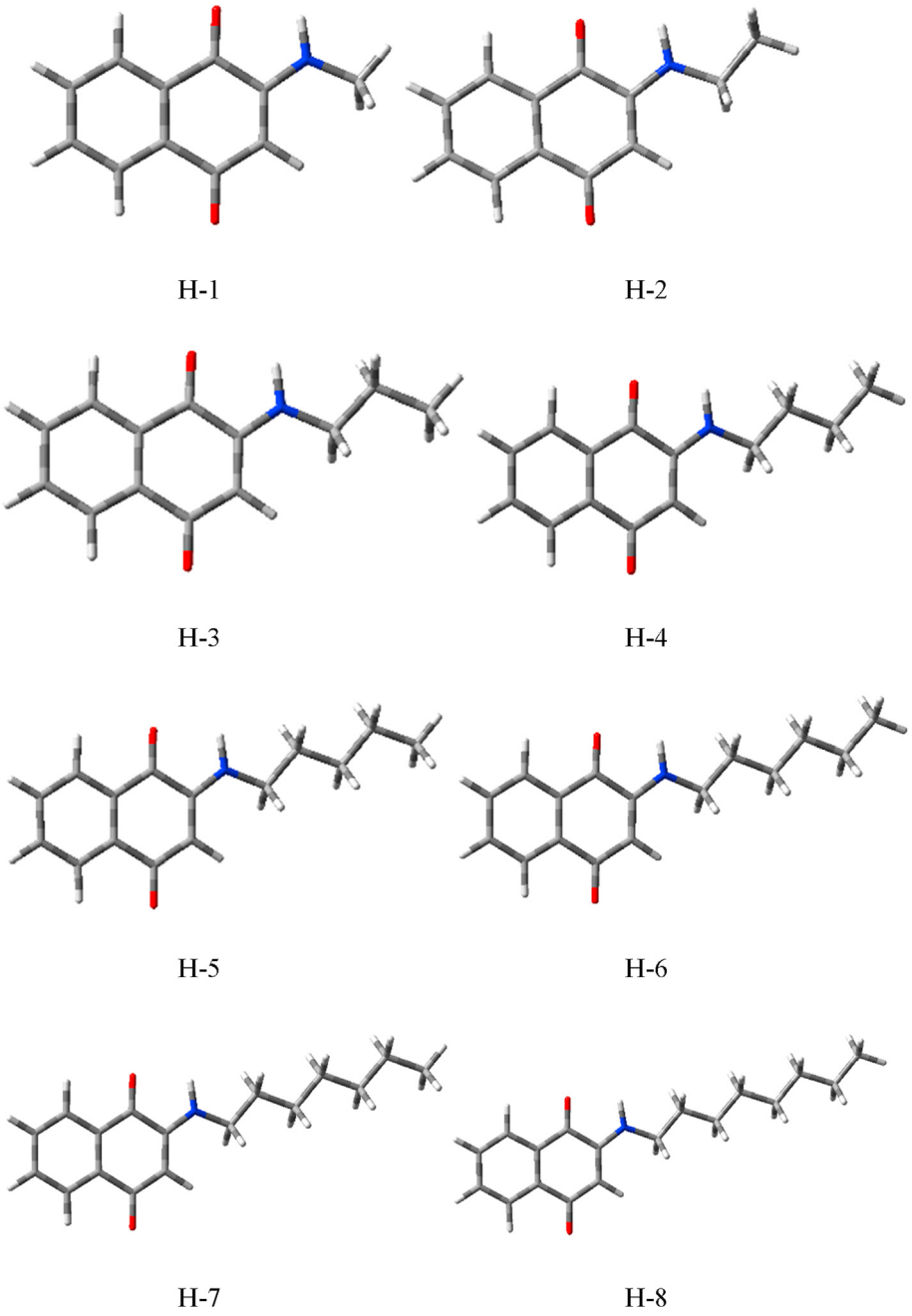

Figure 4. DFT structures of the 2-(*n*-alkylamino)-naphthalene-1,4-dione derivatives H-1 to H-7.

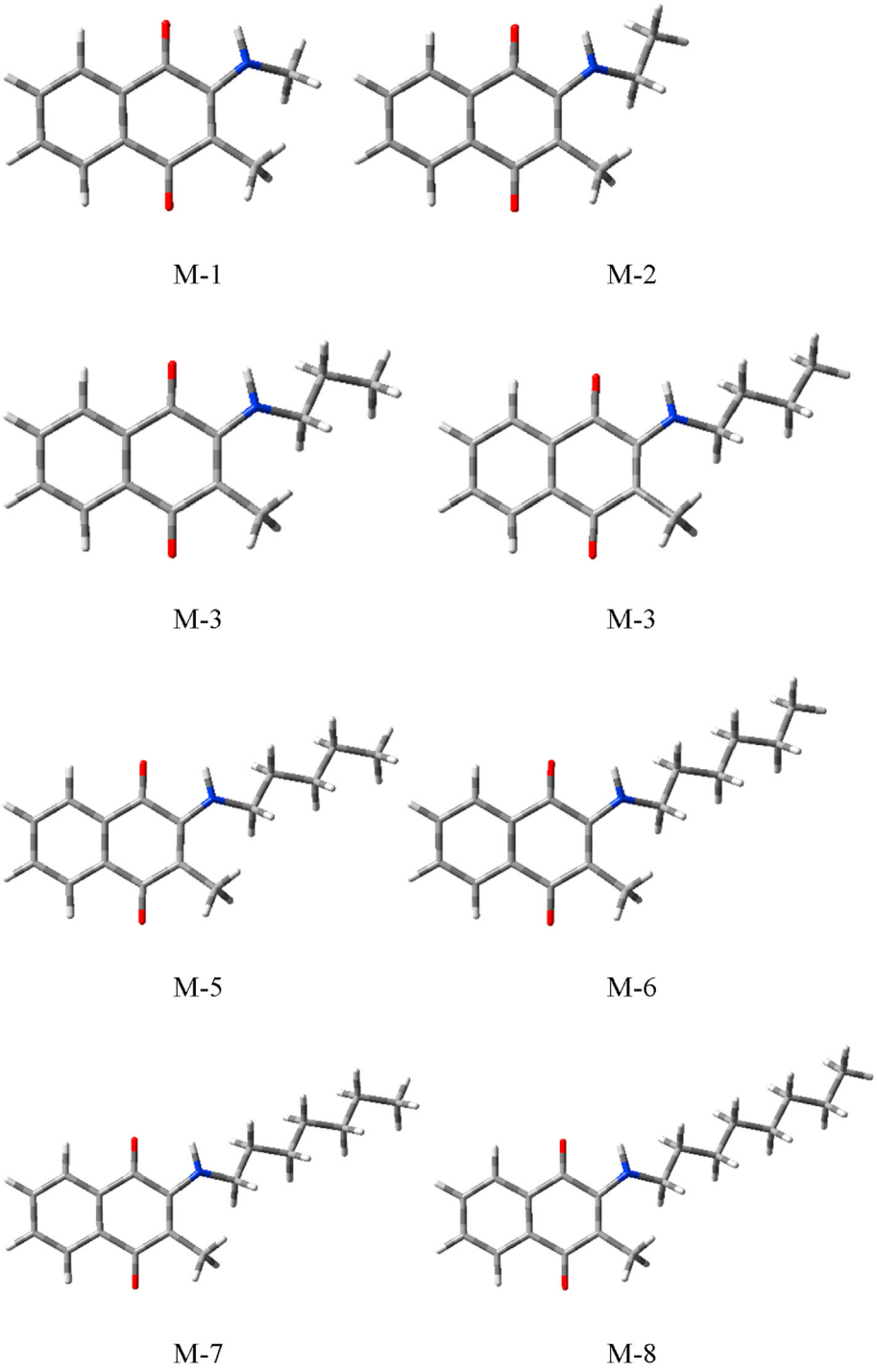

Figure 5. DFT structures of the 2-(*n*-alkylamino)-3-methyl-naphthalene-1,4-dione derivatives M-1 to M-8.

downfield for Cl-2 to Cl-6 and Cl-8 (at ~ δ = 167 ppm) was observed. A major difference was noticed in the ^{13}C chemical shift of carbon, C(3). In the case of C(3), unsubstituted compounds H-1 to H-8 appear at ~ δ = 99 ppm, whereas the corresponding downfield shifts with δ being 110 ppm and 129 ppm, respectively, were noticed along M-1 to M-8 and Br-1 to Br-8 series. The differences observed in the carbon's chemical shift at C(2) and C(3) accounted for the electronegativity differences at these positions. The ^{13}C chemical shift of *n*-alkylamino carbons of analogs compounds was found in a similar range except for the terminal methyl carbons of first two analogs of each series.

The variation in chemical shift can be correlated to hydrogen bond strength (intra & intermolecular) and the presence of electronegative substituent at C(3). After overlapping the single-crystal data of the H-2, Br-2, and Cl-2, it is transparent that there is a change in orientations of the alkyl chain due to electronegative substituent at C(3) position [29, 47]. Similar were the observations in the overlay structures of Cl-6 and

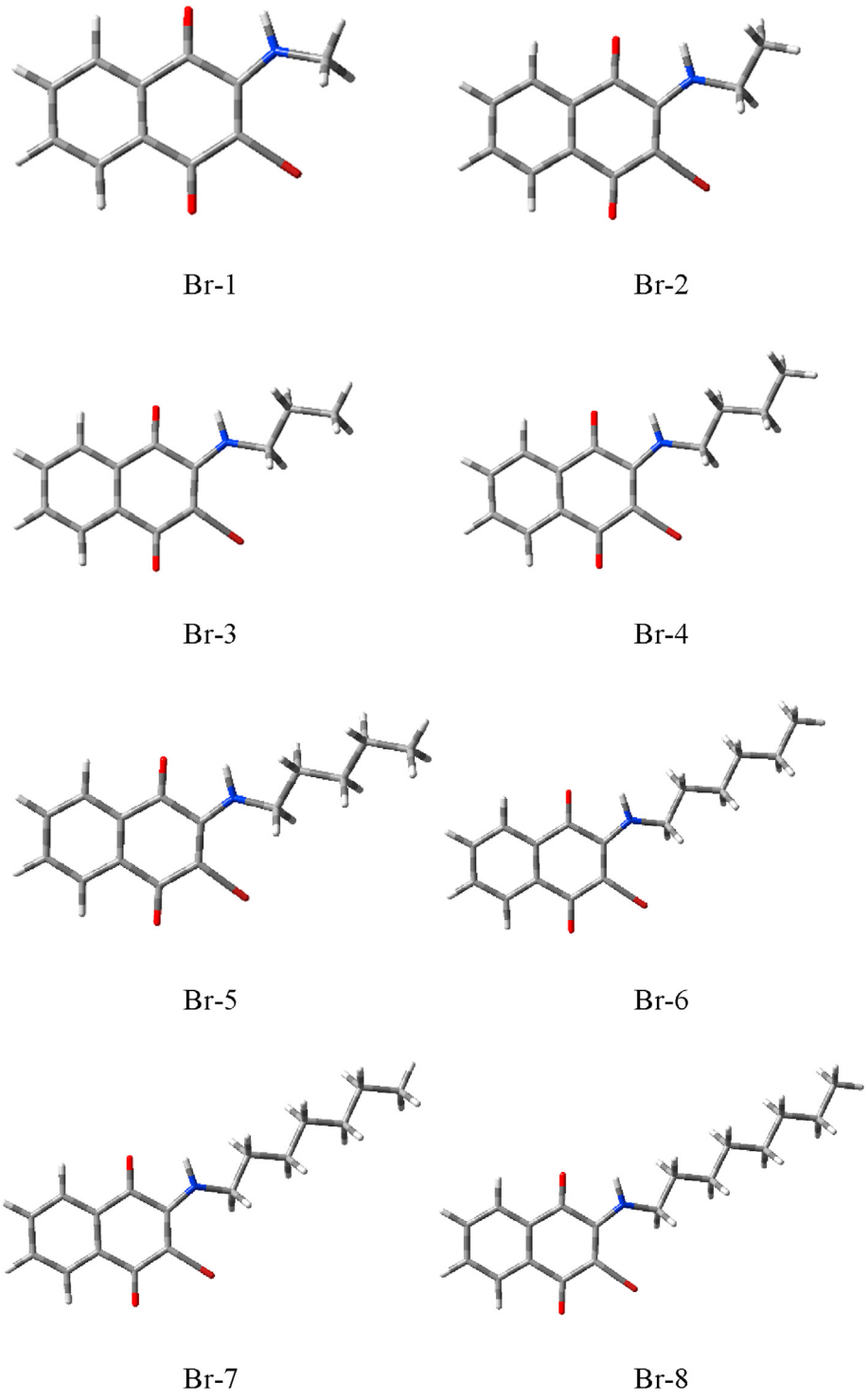

Figure 6. DFT structures of the 2-(*n*-alkylamino)-3-bromo-naphthalene-1,4-dione derivatives Br-1 to Br-8.

H-6. Thus the single-crystal X-ray diffraction studies were performed for all the synthesized derivatives to as certain the effect of structural change in variation of chemical shifts along homologated series [32].

3.3. DFT investigations

Energy-minimal optimized geometrical configurations of alkylamino derivatives with methyl, chlorine, and bromine substituted at C(3) positions within the M06-2X/6-311++G (d,p) density functional framework are depicted in Figures 4, 5, 6 and 7 [36,44]. ^{1}H NMR chemical shifts (δH) were simulated through the SCRF-PCM theory and are reported in Tables 3, 4, and 5. As can be noticed from the table, the alkyl protons emerge with up-field δ_H signals. In contrast, the aromatic proton is relatively de-shielded in the calculated ^{1}H NMR for all alkylamino derivatives. The NH proton shows a signal ~6.16 ppm in the compound molecule upon increasing the alkyl chain from methyl to

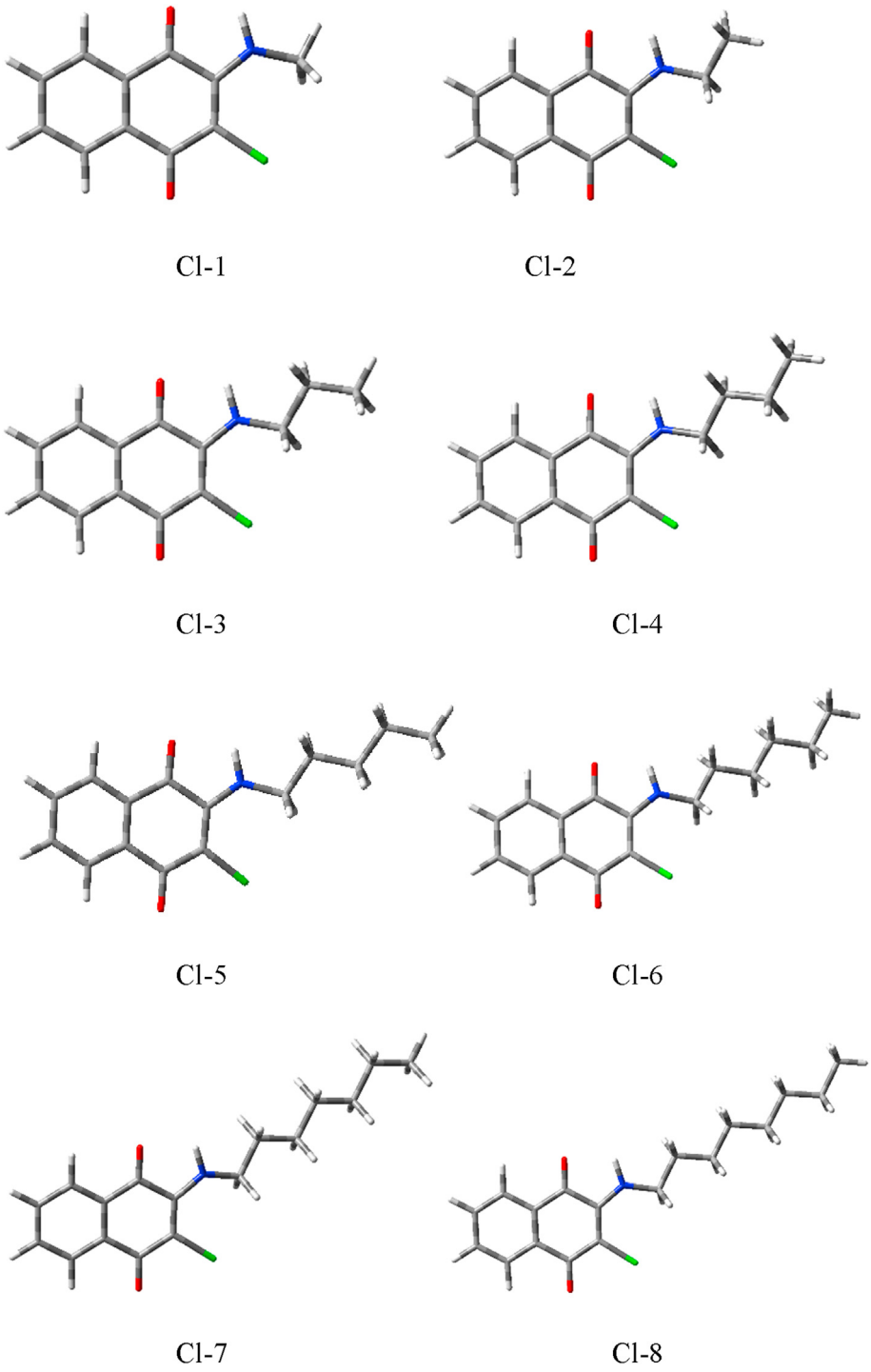

Figure 7. DFT structures of the 2-(*n*-alkylamino)-3-chloro-naphthalene-1,4-dione derivatives Cl-1 to Cl-8.

octyl; it is observed that the chemical shift value decreases up to 0.08 ppm. Similar inferences are drawn for methyl, chlorine, and bromine series of compounds (see Figures 5 and 6).

4. Conclusions

Chloro, bromo, methyl, and proton derivatives of eight analogs of homologated series 2-(*n*-alkylamino)-3R-naphthalene-1,4-dione (where *n*-alkyl = methyl to octyl and R = –H, –CH_3, -Br and -Cl) were analyzed by using the NMR spectroscopy. The ^{1}H and ^{13}C NMR chemical shifts of 32 compounds were assigned, and a comparison has been made. A considerable variation along the chloro, bromo unsubstituted and methyl derivatives was observed. The C(1), C(2), and C(3) carbons show a significant variation in the chemical shift values of ^{13}C NMR spectra. The difference in the chemical shift observed along H-1 to H-8, M-1 to M-8, Br-1 to Br-8, and Cl-1 to the Cl-8 series of compounds. The ^{1}H NMR

chemical shift values are compared with the theoretical NMR values calculated from the DFT calculations. The experimental values show shifting towards the lower, whereas the computed values show higher values.

Declarations

Author contribution statement

Rishikesh Patil: Conceived and designed the experiments; Performed the experiments; Analyzed and interpreted the data.

Mahesh Jadhav: Analyzed and interpreted the data.

Sunita Salunke-Gawali: Conceived and designed the experiments; Analyzed and interpreted the data; Contributed reagents, materials, analysis tools or data; Wrote the paper.

Dipali N. Lande: Performed the experiments; Analyzed and interpreted the data.

Shridhar P. Gejji: Analyzed and interpreted the data; Contributed reagents, materials, analysis tools or data.

Debamitra Chakravarty: Performed the experiments.

Funding statement

Sunita Salunke-Gawali was supported by the Science and Engineering Research Board, Department of Science and Technology, India (EMR/2016/007912). Shridhar Gejji was supported by the Board of Research in Nuclear Sciences, India (v37 (2)/14/11/2015-BRNS). Dipali Lande was supported by University Grants Commission, India.

Data availability statement

Data included in article/supplementary material/referenced in article.

Declaration of interests statement

The authors declare no conflict of interest.

Additional information

Supplementary content related to this article has been published online at https://doi.org/10.1016/j.heliyon.2021.e06044.

Acknowledgements

SPG thanks the Centre for Development of Advanced Computing (C-DAC), Pune, India for computer time at the National Param Super-computing Facility.

References

[1] W. Kellerschierlein, M. Meyer, L. Cellai, D. Lamba, A. Segre, W. Fedeli, M. Brufani, Metabolites of microorganisms. 229, Absolute configuration of naphthomycin a determined by X-ray analysis and chemical degradation, J. Antibiot. 37 (1984) 1357–1361.

[2] C. Lu, Y. Shen, A novel ansamycin, naphthomycin K from Streptomyces sp, J. Antibiot. 60 (2007) 649–653.

[3] M.C. Wilson, S.-J. Nam, T.A.M. Gulder, C.A. Kauffman, P.R. Jensen, W. Fenical, B.S. Moore, Structure and biosynthesis of the marine streptomycete ansamycin ansalactam A and its distinctive branched chain polyketide extender unit, J. Am. Chem. Soc. 133 (2011) 1971–1977.

[4] L. Ding, A. Maier, H.-H. Fiebig, H. Görls, W.-H. Lin, G. Peschel, C. Hertweck, Divergolides A–D from a mangrove endophyte reveal an unparalleled plasticity in ansa-macrolide biosynthesis, Angew. Chem. Int. Ed. 50 (2011) 1630–1634.

[5] Q. Kang, Y. Shen, L. Bai, Biosynthesis of 3,5-AHBA-derived natural products, Nat. Prod. Rep. 29 (2012) 243–263.

[6] E.A. Vasileva, N.P. Mishchenko, P. Zadorozhny, S. A Fedoreyev, New Aminonaphthoquinone from the sea urchins Strongylocentrotus pallidus and Mesocentrotus nudus, Nat. Prod. Commun. 11 (2016) 821–824.

[7] K. Xu, Z. Xiao, Y.B. Tang, L. Huang, C.H. Chen, E. Ohkoshi, K.H. Lee, Design and synthesis of naphthoquinone derivatives as antiproliferative agents and 20S proteasome inhibitors, Biorg. Med. Chem. Lett. 22 (2012) 2772–2774.

[8] E.S. Inks, B.J. Josey, S.R. Jesinkey, C.J. Chou, A novel class of small molecule inhibitors of HDAC6, ACS Chem. Biol. 7 (2012) 331–339.

[9] K. Tatsuta, Total synthesis of the big four antibiotics and related antibiotics, J. Antibiot. 66 (2013) 107–129.

[10] K.W. Wellington, Understanding cancer and the anticancer activities of naphthoquinones – a review, RSC Adv. 5 (2015) 20309–20338.

[11] S.T. Huang, H.S. Kuo, C.L. Hsiao, Y.L. Lin, Efficient synthesis of 'redox-switched' naphthoquinone thiol-crown ethers and their biological activity evaluation, Bioorg. Med. Chem. 10 (2002) 1947–1952.

[12] S.N. Sunassee, C.G.L. Veale, N. Shunmoogam-Gounden, O. Osoniyi, D.T. Hendricks, M.R. Caira, J.A. De La Mare, A.L. Edkins, A.V. Pinto, E.N. Da Silva Júnior, M.T. Davies-Coleman, Cytotoxicity of lapachol, β-lapachone and related synthetic 1,4-naphthoquinones against oesophageal cancer cells, Eur. J. Med. Chem. 62 (2013) 98–110.

[13] A.E. Souza, D.V. Figueiredo, A. Esteves, C.A. Camara, M.D. Vargas, A.C. Pinto, A. Echevarria, Cytotoxic and DNA-topoisomerase effects of lapachol amine derivatives and interactions with DNA, Braz. J. Med. Biol. Res. 40 (2007) 1399.

[14] K.M. Oliveira, L.D. Liany, R.S. Corrêa, V.M. Deflon, M.R. Cominetti, A.A. Batista, Selective Ru(II)/lawsone complexes inhibiting tumor cell growth by apoptosis, J. Inorg. Biochem. 176 (2017) 66–76.

[15] J.J. Inbaraj, C.F. Chignell, Cytotoxic action of juglone and plumbagin: A mechanistic study using HaCaT keratinocytes, Chem. Res. Toxicol. 17 (2004) 55–62.

[16] J.S. Novais, V.R. Campos, A.C.J.A. Silva, M.C.B.V. de Souza, V.F. Ferreira, V.G.L. Keller, M.O. Ferreira, F.R.F. Dias, M.I. Vitorino, P.C. Sathler, M.V. Santana, J.A.L.C. Resende, H.C. Castroa, A.C. Cunha, Synthesis and antimicrobial evaluation of promising 7-arylamino-5,8-dioxo-5,8-dihydroisoquinoline-4-carboxylates and their halogenated amino compounds for treating Gram-negative bacterial infections, RSC Adv. 7 (2017) 18311–18320.

[17] T. Furumoto, Biosynthetic origin of 2,3-Epoxysesamone in a Sesamum indicum hairy root culture, Biosci. Biotechnol. Biochem. 73 (2009) 2535–2537.

[18] Q. Li, C. Khosla, J.D. Puglisi, C.W. Liu, Solution structure and backbone dynamics of the holo form of the frenolicin acyl carrier protein, Biochemistry 42 (2003) 4648–4657.

[19] A.T. Dharmaraja, T.K. Dash, V.B. Konkimalla, H. Chakrapani, Synthesis, thiol-mediated reactive oxygen species generation profiles and anti-proliferative activities of 2,3-epoxy-1,4-naphthoquinones, Med. Chem. Commun. 3 (2012) 219–224.

[20] M. Jeya, H.J. Moon, J.L. Lee, I.W. Kim, J.K. Lee, Current state of coenzyme Q10 production and its applications, Appl. Microbiol. Biotechnol. 85 (2010) 1653–1663.

[21] R.A. Illos, E. Harlev, S. Bittner, A novel all-organic chemical and electrochemical fluorescent switch, Tetrahedron Lett. 46 (2005) 8427–8430.

[22] P. Mande, E. Mathew, S. Chitrambalam, I.H. Joe, N. Sekar, NLO properties of 1, 4-naphthoquinone, Juglone and Lawsone by DFT and Z-scan technique – A detailed study, Opt. Mater. 72 (2017) 549–558.

[23] E. Navarro-García, M.D. Velasco, F. Zapata, A. Bauzá, A. Frontera, C.R. de Arellano, A. Caballero, Exploiting 1,4-naphthoquinone and 3-iodo-1,4- naphthoquinone motifs as anion binding sites by hydrogen or halogen-bonding interactions, Dalton Trans. 48 (2019) 11813–11821.

[24] F.W. Ribeiro, M.C.F.R. Pinto, A.V. Pinto, C.G.T. De Oliveira, V.F. Ferreira, ^{13}C - Nuclear Magnetic Resonance study of 1,2 - and 1,4 naphthoquinones and their derivatives, J. Braz. Chem. Soc. 1 (1990) 55–57.

[25] E. Bedir, A.M.S. Pereira, S.I. Khan, A. Chittiboyina, R.M. Moraes, I.A. Khan, A new β-lapachone derivative from *Distictella elongata* (Vahl) Urb. J. Braz. Chem. Soc. 20 (2009) 383–386.

[26] M. Higa, N. Noha, H. Yokaryo, K. Ogihara, S. Yogi, Three new naphthoquinone derivatives from Diospyros maritima Blume, Chem. Pharm. Bull. 50 (2002) 590–593.

[27] V. Prezhdo, E. Ovsiankina, O. Prezhdo, Conformational analysis of chloroalkyl derivatives of 1,4-naphthoquinone, J. Mol. Struct. 522 (2000) 71–77.

[28] O. Pawar, A. Patekar, A. Khan, L. Kathawate, S. Haram, G. Markad, V. Puranik, S. Salunke-Gawali, Molecular structures and biological evaluation of 2-chloro-3-(n-alkylamino)-1,4-napthoquinone derivatives as potent antifungal agents, J. Mol. Struct. 1059 (2014) 68–74.

[29] S. Salunke-Gawali, O. Pawar, M. Nikalje, R. Patil, T. Weyhermüller, V.G. Puranik, V.B. Konkimalla, Synthesis, characterization and molecular structures of homologated analogs of 2-bromo-3-(n-alkylamino)-1,4-napthoquinone, J. Mol. Struct. 1056–1057 (2014) 97–103.

[30] D. Chadar, M. Camilles, R. Patil, A. Khan, T. Weyhermüller, S. Salunke-Gawali, Synthesis and characterization of n-alkylamino derivatives of vitamin K3: Molecular structure of 2-propylamino-3-methyl-1,4-naphthoquinone and antibacterial activities, J. Mol. Struct. 1086 (2015) 179–189.

[31] D. Chadar, P. Banerjee, S. Kr. Saha, S. Bhand, R. Patil, S. Salunke-Gawali, n-alkylamino analogs of Vitamin K3: Electrochemical, DFT and anticancer activity of their oxidized and one electron reduced form, J. Mol. Struct. 1179 (2019) 443–452.

[32] R. Patil, D. Chadar, D. Chaudhari, J. Peter, M. Nikalje, T. Weyhermüller, S. Salunke Gawali, Synthesis and characterization of 2-(n-alkylamino)-1,4-napthoquinone: Molecular structures of ethyl and hexyl derivatives, J. Mol. Struct. 1075 (2014) 345–351.

[33] R. Patil, S. Bhand, B. Konkimalla, P. Banerjee, B. Ugale, D. Chadar, S. Saha, P.P. Praharaj, C.M. Nagaraja, D. Chakrovarty, S. Salunke-Gawali, Molecular association of 2-(n-alkylamino)-1,4-naphthoquinone derivatives: Electrochemical,

DFT studies and antiproliferative activity against leukemia cell lines, J. Mol. Struct. 1125 (2016) 272–281.
[34] S. Pal, M. Jadhav, T. Weyhermüller, Y. Patil, M. Nethaji, U. Kasabe, L. Kathawate, V.B. Konkimalla, S. Salunke-Gawali, Molecular structures and antiproliferative activity of side-chain saturated and homologated analogs of 2-chloro-3-(n-alkylamino)-1,4-napthoquinone, J. Mol. Struct. 1049 (2013) 355–361.
[35] D.D. Perrin, W.L. Armarego, D.R. Perrin, Purification of Laboratory Chemicals, Pergamon Press, London, 1988, p. 260.
[36] A. Patil, D. Lande, A. Nalkar, S. Gejji, D. Chakravarty, R. Gonnade, T. Moniz, M. Rangel, E. Pereira, S. Salunke-Gawali, Binding selectivity of vitamin K3 based chemosensors towards nickel(II) and copper(II) metal ions, J. Mol. Struct. 1143 (2017) 495–514.
[37] S. Gorohovsky, G. Temtsin-Krayz, S. Bittner, Synthesis of N-quinonyltaurines, Amino Acids 24 (2003) 281–287.
[38] L. Pan, Q. Zheng, Y. Chen, R. Yang, Y. Yang, Z. Li, X. Meng, Design, synthesis and biological evaluation of novel naphthoquinone derivatives as IDO1 inhibitors, Eur. J. Med. Chem. 157 (2018) 423–436.
[39] A.P.E.X.2 Bruker, SAINT and SADABS, Bruker AXS Inc, Madison, Wisconsin, USA, 2007.
[40] G.M. Sheldrick, A short history of SHELX, Acta Crystallogr. A64 (2008) 112–122.
[41] C.F. Macrae, I.J. Bruno, J.A. Chisholm, P.R. Edgington, P. McCabe, E. Pidcock, L.R. Monge, R. Taylor, J. van de Streek, P.A. Wood, Mercury CSD 2.0—new features for the visualization and investigation of crystal structures, J. Appl. Crystallogr. 41 (2008) 466–470.
[42] L. Spek, Structure validation in chemical crystallography, Acta Crystallogr. D65 (2009) 148–155.
[43] P. Gosavi-Mirkute, A. Patil, D.N. Lande, D. Chakravarty, S.P. Gejji, S. Satpute, S. Salunke-Gawali, Naphthoquinone based chemosensors for transition metal ions: experiment and theory, RSC Adv. 7 (2017) 55163–55174.
[44] D. Choudhari, D. Lande, D. Chakravarty, S. Gejji, Parijat Das, K. Pardesi, S. Satpute, S. Salunke-Gawali, Reactions of 2,3-dichloro-1,4-naphthoquinone with aminophenols: evidence for hydroxy benzophenoxazine intermediate and antibacterial activity, J. Mol. Struct. 1176 (2019) 194–206.
[45] E. Leyva, K.M. Baines, C.G.E. González, D.A. Magaldi-Lara, S.E. Loredo-Carrillo, T.A. de Luna-Méndez, L.I. López, 2-(Fluoro-) and 2-(methoxyanilino)-1,4-naphthoquinones. Synthesis and mechanism and effect of fluorine substitution on redox reactivity and NMR, J. Fluor. Chem. 180 (2015) 152–160.
[46] M.A. Elsayed, M.E. Abdel-hamid, M.A. Korany, M.H. Abdel-hay, S.M. Galal, Spectroscopic investigation of the Antazoune-p-chloranilic acid reaction product, 12 17 (1984) 803–818.
[47] S. Bhand, R. Patil, Y. Shinde, D. Lande, S. Rao, L. Kathawate, S. Gejji, T. Weyhermuller, S. Salunke-Gawali, Tautomerism in o-hydroxyanilino-1,4-naphthoquinone derivatives: Structure, NMR, HPLC and density functional theoretic investigations, J. Mol. Struct. 1123 (2016) 245–260.